

Low-Profile Broadband Dual-Polarized Dipole Antenna on AMC Reflector for Base Station

Bin Wang, Cencen Huang*, Wei Luo, and Wei Ruan

Abstract—Artificial magnetic conductor (AMC) is a periodic structure with in-phase reflection, which can be used in dual-polarization dipole antenna to reduce profile height. In this study, a low-profile dual-polarized dipole antenna with an AMC reflector is proposed by improving the AMC structure. The antenna consists of a pair of orthogonal planar dipoles with U-shaped slots, two T-shaped feeding lines, and an AMC reflector. The overall height is $0.132\lambda_{2.2\text{GHz}}$. Experimental results show that the proposed antenna has a wider bandwidth than other antennas of the same type. The impedance bandwidth of this antenna is 52% (1.65 GHz to 2.81 GHz), and the proposed antenna also has the advantages of low profile, high port isolation (< -30 dB), and low cross polarization (< -27 dB). These features can meet the current needs of the telecommunications industry.

1. INTRODUCTION

The demand of wireless information transmission gradually increases the complexity of communication systems. Base station antenna is developing toward dual polarizations, broadband, and miniaturization, which is the tendency of 5G communication technology research, to adapt to the long-term coexistence of many mobile communication standards and to solve the current tension situation of base station sector position. Conventional dual-polarized antennas generally can be achieved by microstrip patch antennas or dipole antennas, and each has its own advantages and disadvantages. The microstrip patch antennas [1–3] have a low-profile characteristic, but their application in the base station is restricted because of their narrow bandwidth and big loss. The dipole antennas [4–6] can always be designed reasonably to meet the current mobile communication requirements of bandwidth. In [7], the antenna utilizes two crossed planar bow-tie dipoles to achieve $\pm 45^\circ$ dual polarizations, which has an impedance bandwidth of 45% for $\text{VSWR} < 1.5$, and the isolation between the two ports is more than 30 dB. Dipole antennas need to be placed $\lambda/4$ above a perfect electric conductor (PEC) to obtain a good performance. Such a high profile does not conform to the trend of miniaturization of base stations. Therefore, the study of broadband miniaturization of dual-polarized antennas has become a research hot spot. In essence, the general methods of miniaturization are to take a dielectric substrate with a high dielectric constant [8], extend path of flowing [9, 10] and to introduce reactance elements [11] or shorting probes [12]. But the effect of these methods on miniaturization of dual-polarized dipole antennas is not obvious. The miniaturization design of dual-polarized dipole antennas is intended to lower the profile or to reduce the lateral area. As a special electromagnetic material, artificial magnetic conductor (AMC) structure provides a way to lower the profile of dipole antennas. Several different AMCs are investigated in terms of their reflection phase characteristics versus frequency in [13]. However, the in-phase reflection bandwidth of AMC structure is narrow; thus, a wide band with dipole antenna is difficult to obtain. The AMC structure is used to effectively improved the performances of folded dipole antenna in [14, 15].

Received 21 March 2017, Accepted 26 May 2017, Scheduled 1 June 2017

* Corresponding author: Cencen Huang (huangcencen108@163.com).

The authors are with the College of Electronic Engineering, Chongqing University of Posts and Telecommunications, Chongqing, China.

[16, 17] load a circular polarization antenna into the AMC structure, which can be applied to wireless frequency bands, respectively. The performance of a periodic patch with a rectangular ring and a pair of bending lines presented in [18] is significantly good. The dual-polarized antenna with this AMC structure can obtain a bandwidth of 35%. Nevertheless, the structure is relatively complex. In [19], the traditional mushroom-type AMC structure is used as a dual-polarized antenna reflector to effectively reduce the height. The impedance bandwidth, however, is only 18.7% for $VSWR < 2$.

In this study, a low-profile dual-polarized dipole antenna with an AMC reflector is proposed in combination with the design requirements of dual polarizations, broadband, and miniaturization. In our previous study, we designed a broadband dual-polarized dipole antenna with metallic cylinder for base station [20]. Nevertheless, the height of this antenna is approximately $0.264\lambda_{2.2\text{ GHz}}$. On this basis, an improved AMC structure is proposed in the current study. The improved structure replaces the original metal reflector and effectively reduces the antenna profile while maintaining its good characteristics. Furthermore, compared with the other same type antennas, the proposed antenna can achieve wider bandwidth. A detailed comparison between the references and proposed antenna is listed in Table 1. The measurement results show that the antenna has the advantages of low profile, broadband, high isolation, and low cross polarization. These characteristics collectively meet the current standards of the mobile communication industry.

Table 1. A comparison between the reference and proposed antenna.

Ref.	Polarization	Thickness, mm	Bandwidth
[14]	Linearly polarized	$0.059\lambda_{5.5\text{ GHz}}$	6% (5.34 GHz–5.67 GHz)
[15]	Linearly polarized	$0.129\lambda_{5.7\text{ GHz}}$	31.6% (4.8 GHz–6.6 GHz)
[16]	Circularly polarized	$0.053\lambda_{1.65\text{ GHz}}$	18.8% (1.49 GHz–1.8 GHz)
[18]	Dual-polarized	$0.083\lambda_{0.83\text{ GHz}}$	35% (678 MHz–965 MHz)
[19]	Dual-polarized	$0.134\lambda_{2.5\text{ GHz}}$	18.7% (2.28 GHz–2.75 GHz)
Proposed antenna	Dual-polarized	$0.132\lambda_{2.2\text{ GHz}}$	52% (1.65 GHz–2.81 GHz)

2. ANTENNA DESIGN

The configuration of the proposed dual-polarized antenna with an AMC reflector is shown in Fig. 1. The overall height is $0.132\lambda_{2.2\text{ GHz}}$. The AMC reflector consists of 11×11 units. The plane dipole antenna is supported by four plastic columns above the AMC reflector. The details are as follows.

2.1. Geometry of Plane Dipole Antenna

Figure 2 presents the geometry of plane dipole antenna. (a) and (b) are respectively etched onto the up-down layer of an FR4 substrate with a dielectric constant of 4.4, loss tangent of 0.02, and thickness of 0.5 mm. As radiators of the antenna, two planar dipoles (the red one and the blue one) are placed orthogonally on the lower layer of the FR4 substrate to configure for $\pm 45^\circ$ polarization diversity. The one reason why the antenna obtains a wide bandwidth is the mutual coupling between the two dipoles. Each dipole arm is formed by an isosceles trapezoid $A'B'C'D'$ and a semicircle $A'O'B'$. The U-shaped slots embedded within the dipole arms are used to improve the impedance matching by changing the path of current flowing through the dipole arm. The T-shaped feeding lines associated with the dipoles are placed perpendicularly on the upper layer of the FR4 substrate. The design of air bridge is used considerably to avoid the overlap of the two T-shaped feeding lines in physical position. The radiators are coupled by the T-shaped feeding lines that are directly fed by two coaxial cables. The feeding structure is shown in (b). The distance between the planar dipole antenna and the AMC reflector is 4.5 mm.

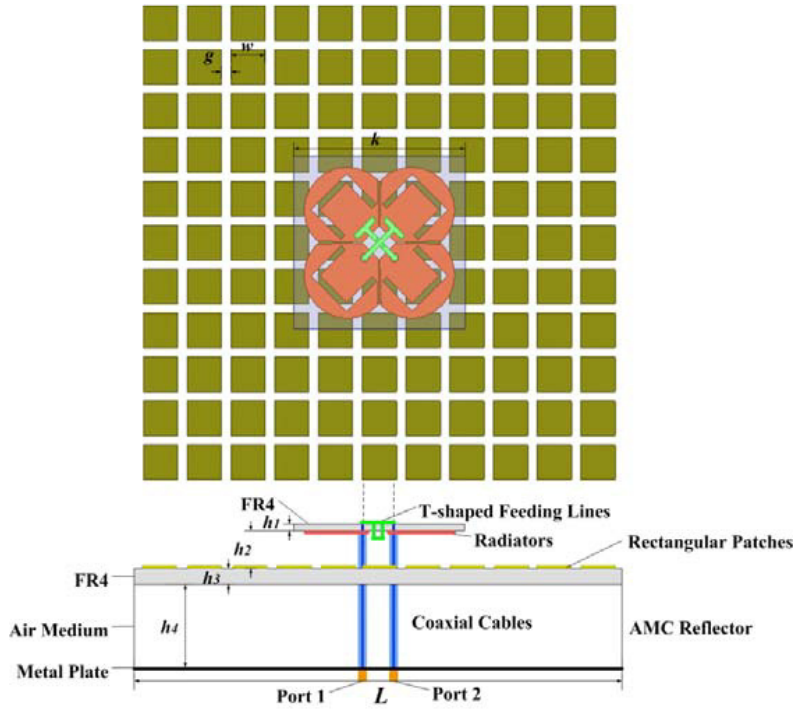


Figure 1. Configuration of the proposed dual-polarized antenna with an AMC reflector.

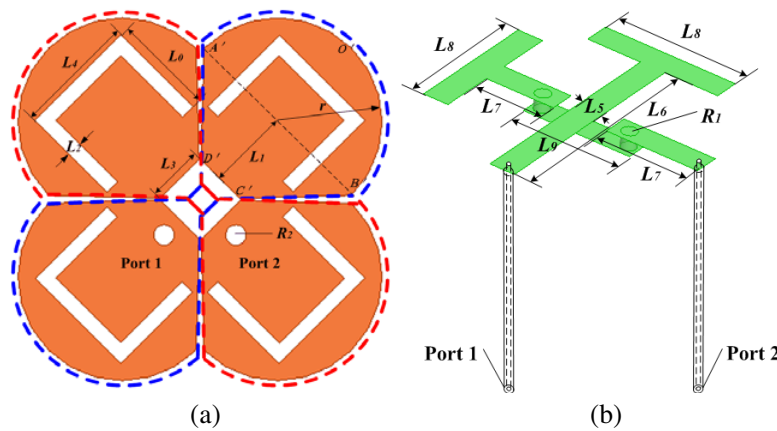


Figure 2. Geometry of plane dipole antenna. (a) Radiator of the antenna. (b) Feeding structure of the antenna.

3. DESIGN OF THE AMC REFLECTOR

In this study, an AMC structure without conducting vias is designed. On the basis of the typical mushroom-type AMC structure proposed in [21], the frequency range of the reflection phase from -90° to $+90^\circ$ is defined as the in-phase reflection bandwidth of the AMC structure. The traditional mushroom-type AMC structure usually has a high work frequency and a narrow in-phase reflection bandwidth. This AMC structure cannot meet the design requirements of telecommunication base stations. So it is necessary to improve the traditional mushroom-type AMC structure to cover frequency needed for communication. The AMC structure without conducting vias and its LC equivalent circuit are presented in Fig. 3, where w_r is the side length of the square patch, g_r the gap width among adjacent cells, h_r the thickness of the dielectric substrate, and ϵ_r the dielectric constant for the dielectric substrate.

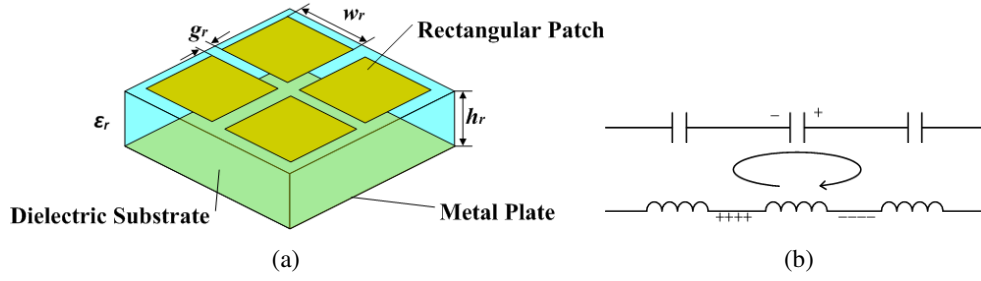


Figure 3. AMC structure without conducting vias and its LC equivalent circuit. (a) AMC structure without conducting vias. (b) LC equivalent circuit.

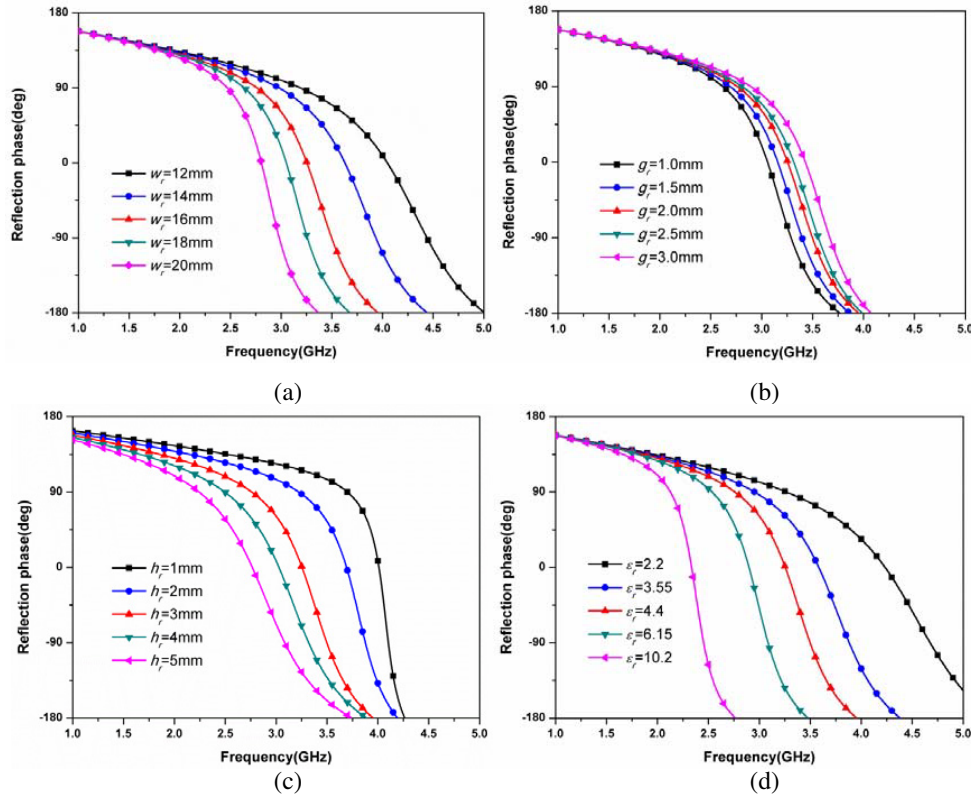


Figure 4. Effects of the main parameters of the AMC structure on the reflection phase. (a) Simulated reflection phase for different w_r . ($g_r = 2$ mm, $h_r = 3$ mm, $\varepsilon_r = 4.4$). (b) Simulated reflection phase for different g_r . ($w_r = 16$ mm, $h_r = 3$ mm, $\varepsilon_r = 4.4$). (c) Simulated reflection phase for different h_r . ($w_r = 16$ mm, $g_r = 2$ mm, $\varepsilon_r = 4.4$). (d) Simulated reflection phase for different ε_r . ($w_r = 16$ mm, $g_r = 2$ mm, $h_r = 3$ mm).

The main dimensions are set hypothetically as follows: $w_r = 16$ mm, $g_r = 2$ mm, $h_r = 3$ mm, and $\varepsilon_r = 4.4$. The Floquet port method is used to simulate the infinite elements of the AMC structure. The significant effects of the parameters on the reflection phase are indicated in Fig. 4, in which the 0° reflection phase frequency is directly proportional to g_r and is inversely proportional to w_r , h_r , and ε_r . The in-phase reflection bandwidth is directly proportional to g_r and h_r and is inversely proportional to w_r and ε_r . The in-phase reflection bandwidth is inconsiderably affected by the change in g_r but is greatly influenced by changing ε_r .

According to the preceding inferences, the most effective ways to satisfy the characteristics of low work frequency and broadband simultaneously are to increase the thickness of the dielectric substrate

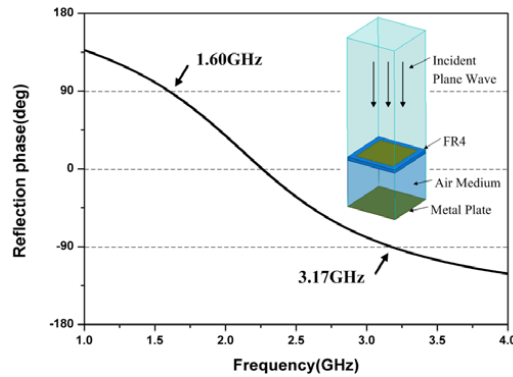


Figure 5. Reflection phase curve of the modified AMC structure.

and to adopt a dielectric substrate with a low dielectric constant. This study creatively replaces the traditional dielectric substrate in the middle with air medium considering the desirability of the processing materials. The top layer of the air medium needs to be realized by the printed circuit board (FR4 substrate with a dielectric constant of 4.4, loss tangent of 0.02, and thickness of 1 mm). The rectangular patches are located in the upper layer of the substrate. The middle is the air medium, and the metal plate is below the air medium. The reflection phase curve is shown in Fig. 5. The optimization of the main parameters ultimately results in 0° reflection phase frequency near 2.2 GHz and the in-phase reflection bandwidth of 1.60 GHz to 3.17 GHz. This modified AMC structure can be used for joint simulation optimization with the planar dipole antenna.

4. SIMULATION AND MEASUREMENT RESULTS

In order to achieve the radiation symmetry of $\pm 45^\circ$ crossed dipole, the proposed antenna still uses the square reflector here. Furthermore, the number of AMC reflector units is studied in quantity to provide a guideline for practical design. Fig. 6 shows the simulated VSWRs and radiation patterns at E -plane of 7×7 units, 9×9 units, 11×11 units and 13×13 units. The result of Fig. 6(b) demonstrates that the half-power beamwidths of 7×7 units, 9×9 units, 11×11 units and 13×13 units are 50° , 62° , 64° and 57° . Synthetically considering the practicality of the base station antennas ($VSWR \leq 1.5$) and the requirement of the half-power beamwidth (the half-power beamwidth at the E -plane and H -plane is approximately 60°), the 11×11 units of the AMC reflector are selected in the final design.

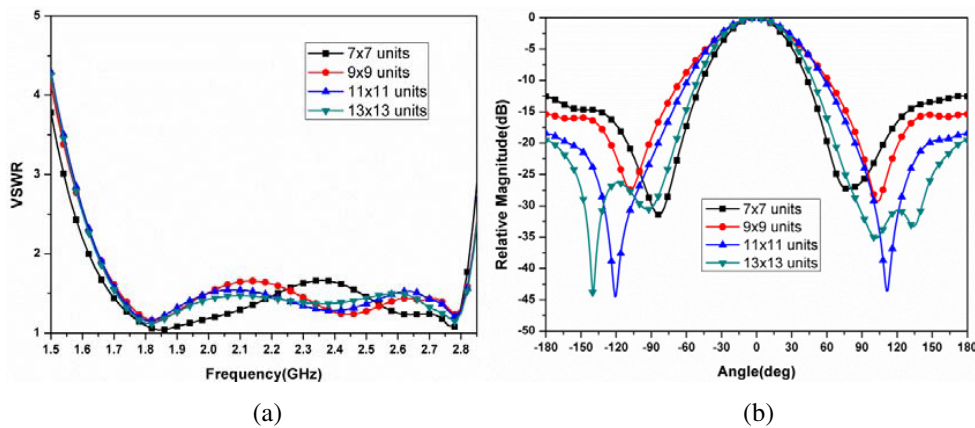


Figure 6. The simulated VSWRs and radiation patterns at E -plane of 7×7 units, 9×9 units, 11×11 units and 13×13 units. (a) The simulated VSWRs of 7×7 units, 9×9 units, 11×11 units and 13×13 units. (b) The radiation patterns at E -plane of 7×7 units, 9×9 units, 11×11 units and 13×13 units.

Table 2. Parameter of the proposed antenna.

Symbol	Value, mm	Symbol	Value, mm
K	60.0	h_1	0.5
h_2	4.5	h_3	1.0
h_4	12.0	L	171.6
L_0	14.7	L_1	11.9
L_2	2.1	L_3	8.0
L_4	17.5	L_5	1.69
L_6	16.0	L_7	6.3
L_8	9.0	L_9	7.5
R_1	0.5	R_2	1.49
r	15.1	g	3.3
w	12.0		

The low-profile dual-polarized antenna is simulated by HFSS 13. It is processed and tested to verify the simulation results. The detailed dimensions for this fabrication are listed in Table 2. The VSWR and isolation are measured by using the vector network analyzer (model N5242A Agilent Technologies). The radiation pattern and gain performance of the proposed antenna are obtained in the anechoic chamber. Moreover, the fabricated antennas and testing environment are presented in Fig. 7. It is observed that the overall height of the antenna with an AMC reflector is significantly reduced in comparison with that of the same antenna with a PEC reflector. The height of the antenna with a PEC reflector is approximately quarter wavelength in [20]. Besides, the height of the antenna with an AMC reflector is half of the height of the antenna with a PEC reflector.



Figure 7. The fabricated antenna and testing environment. (a) Comparison of the antenna with an AMC reflector and the same antenna with a PEC reflector. (b) The testing environment.

Figure 8 shows the simulation and measurement results of VSWR of the two ports with different reflectors. A good agreement exists between the two ports. The measured impedance bandwidth of the antenna with PEC reflector is 56.3% (1.58 GHz–2.82 GHz) for VSWR < 2. Replacing the PEC reflector with an AMC reflector, the impedance bandwidth is still able to cover 1.7 GHz to 2.7 GHz. The simulated impedance bandwidth is 49.2% for VSWR < 1.5 from 1.70 GHz to 2.81 GHz. The measured impedance bandwidth is 52% for VSWR < 2 from 1.65 GHz to 2.81 GHz.

The value of port isolation with PEC reflector is less than -30 dB within 1.7 GHz to 2.7 GHz in Fig. 9. The simulated and measured isolations of the two ports with AMC reflector is also below -30 dB within this operating bandwidth.

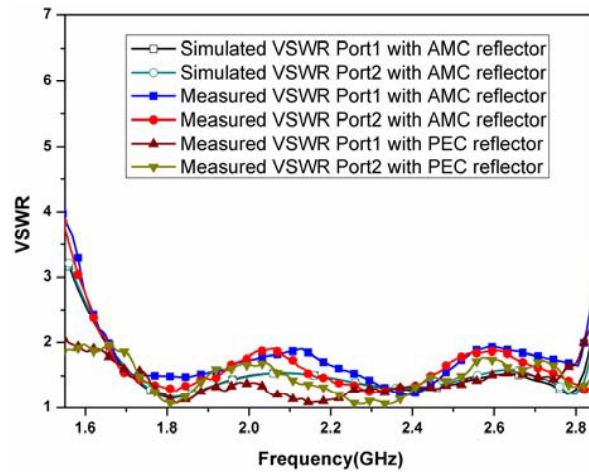


Figure 8. Simulation and measurement results of VSWR of the two ports with different reflectors.

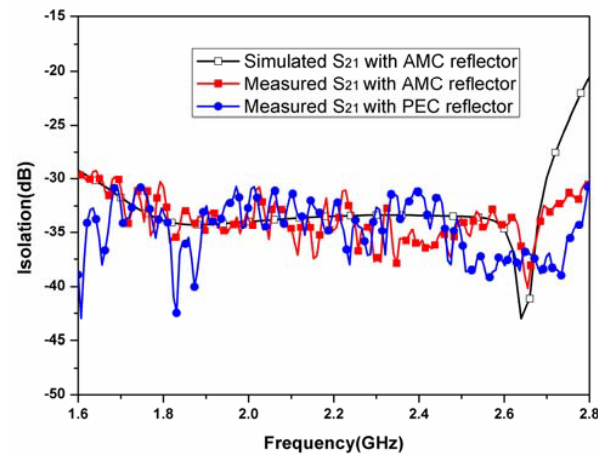


Figure 9. Simulated and measured isolation between the two ports with different reflectors.

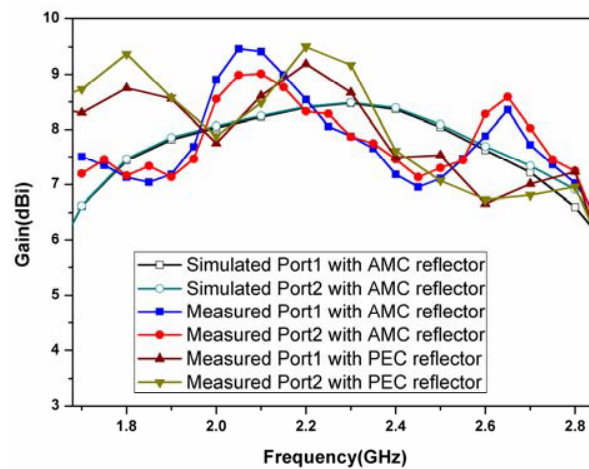


Figure 10. Simulation and measurement results of gain of the two ports with different reflectors.

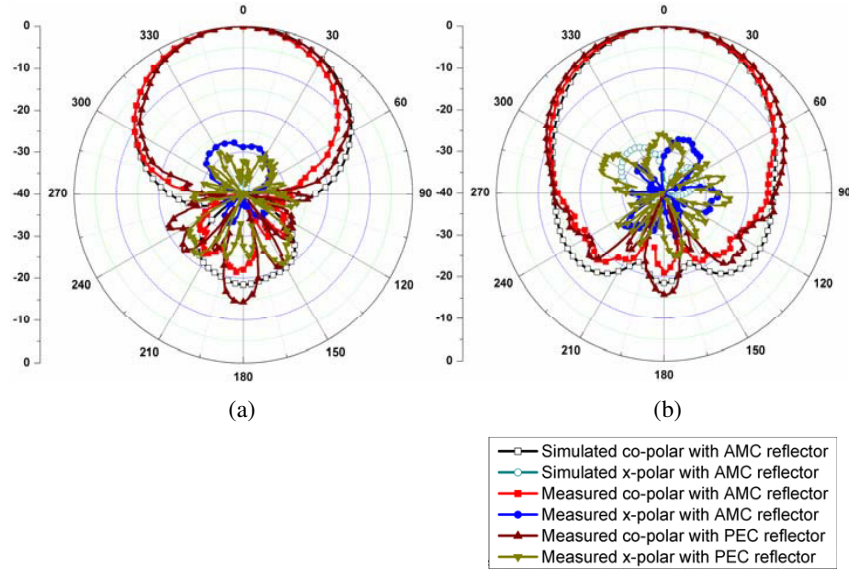


Figure 11. Simulated and measured radiation patterns of the proposed antenna with different reflectors for port 1 at 2.2 GHz. (a) E -plane. (b) H -plane.

As shown in Fig. 10, the simulated curves of the gain in the working frequency band are relatively smooth. Some ripples of the measured results for gain may be caused by the fabrication, assembly and measurement deviation. The simulated average gains of the two ports are both 7.8 dBi. The measured average gains of the two ports are both 7.7 dBi. Moreover, the measured average gains of the antenna with PEC reflector are 8.2 dBi. The gain of the antenna with AMC reflector is slightly reduced, possibly due to the loss of the metal patch on the AMC surface.

The geometric symmetry leads to only one pattern of port 1 in Fig. 11. This figure shows the simulated and measured radiation patterns at frequencies of 2.2 GHz at the E -plane and H -plane. Compared to the radiation patterns with PEC reflector, the antenna with AMC reflector still has good radiation characteristics. The cross polarization on the axis is less than -27 dB, and the half-power beamwidth variation of the antenna at the E -plane and H -plane is $60^\circ \pm 5^\circ$, in good agreement with the simulation results.

As can be seen from the comparisons, the profile of the antenna with AMC reflector is obviously lower than that of the antenna with PEC reflector, and it maintains the same good performance as the latter.

5. CONCLUSION

The miniaturization of a dipole antenna is studied on the basis of previous research. An AMC reflector is used to reduce the overall height of the dual-polarized dipole antenna. The height of the antenna with an AMC reflector is only half of the height of the antenna with a PEC reflector. Nonetheless, the performance of the former antenna is still suitable for the current 1.7 GHz to 2.7 GHz base station applications. The measurement results indicate that the antenna has the advantages of low profile, broadband, high isolation, and low cross polarization. Vertical conducting vias are not integrated into this design, which makes the processing convenient while reducing the manufacturing cost. This study can provide a reference for the miniaturization design of dual-polarized antennas.

REFERENCES

1. Karimkashi, S. and G. Zhang, "A dual-polarization series-fed microstrip antenna array with very high polarization purity for weather measurement," *IEEE Transaction on Antennas and Propagation*, Vol. 61, No. 10, 5315–5319, 2013.

2. Lu, J., Z. Kuai, X. Zhu, and N. Zhang, "A high-isolation dual-polarization microstrip patch antenna with quasi-cross-shaped coupling slot," *IEEE Transaction on Antennas and Propagation*, Vol. 59, No. 7, 2713–2717, 2011.
3. Moradi, K. and S. Nikmehr, "A dual-band dual-polarized microstrip array antenna for base stations," *Progress In Electromagnetics Research*, Vol. 123, 527–541, 2012.
4. Liu, Y., J. Wang, and S. Gong, "Wideband dual-polarized planar antenna for base stations," *Microwave and Optical Technology Lett.*, Vol. 57, No. 8, 1948–1952, 2015.
5. Chu, Q. X., D. L. Wen, and Y. Luo, "A broadband $\pm 45^\circ$ dual-polarized antenna with Y-shaped feeding lines," *IEEE Transaction on Antennas and Propagation*, Vol. 63, No. 2, 483–490, 2015.
6. Feng, B., W. An, S. Yin, L. Deng, and S. Li, "Dual-wideband complementary antenna with a dual-layer cross-ME-dipole structure for 2G/3G/LTE/WLAN applications," *IEEE Antennas and Wireless Propag. Lett.*, Vol. 14, 626–629, 2015.
7. Cui, Y. H., R. L. Li, and H. Z. Fu, "broadband dual-polarized planar antenan for 2G/3G/LTE base stations," *IEEE Transaction on Antennas and Propagation*, Vol. 62, No. 9, 4836–4840, 2014.
8. Sun, M. and Y. P. Zhang, "Miniaturization of planar monopole antennas for ultrawide-band applications," *2007 Int. Workshop on Antenna Technology (iWAT): Small and Smart Antennas Metamaterials and Applications*, 197–200, March 2007.
9. Occhiuzzi, C., C. Paggi, and G. Marrocco, "Passive FRID strain-sensor based on meander-line antennas," *IEEE Transaction on Antennas and Propagation*, Vol. 59, No. 12, 4836–4840, 2011.
10. Ryu, H. K. and J. M. Woo, "Miniaturisation of rectangular loop antenna using meander line for RFID tags," *Electronics Lett.*, Vol. 43, No. 7, 372–374, 2007.
11. Rudant, L. and C. Delaveaud, "Investigation of lumped loading technique for printed antenna miniaturization," *2013 Int. Workshop on Antenna Technology (iWAT)*, 253–256, March 2013.
12. Zuo, S. L., Y. Z. Yin, Z. Y. Zhang, and K. Song, "Enhanced bandwidth of low-profile sleeve monopole antenna for indoor bade station application," *Electronics Lett.*, Vol. 46, No. 24, 1587–1588, 2010.
13. Foroozesh, A. and L. Shafai, "Investigation into the application of artificial magnetic conductors to bandwidth broadening, gain enhancement and beam shaping of low profile and conventional monopole antennas," *IEEE Transaction on Antennas and Propagation*, Vol. 59, No. 1, 4–20, 2011.
14. Vallecchi, A., J. R. D. Luis, F. Capolino, and F. D. Flaviis, "Low profile fully planar folded dipole antenna on a high impedance surface," *IEEE Transaction on Antennas and Propagation*, Vol. 60, No. 1, 51–62, 2012.
15. Li, G., H. Zhai, L. Li, C. Liang, R. Yu, and S. Liu, "AMC-loaded wideband base station antenna for indoor access point in MIMO system," *IEEE Transaction on Antennas and Propagation*, Vol. 63, No. 2, 525–533, 2015.
16. Ta, S. X. and I. Park, "Broadband design of a low-profile, circularly polarized crossed dipole antenna on an AMC surface," *2014 eighth Int. Conf. on Advanced Electromagnetic Materials in Microwaves and Optics (ICAEMMO)*, 238–240, August 2014.
17. Tran, H. H. and I. Park, "A dual-wideband circularly polarized antenna using an artificial magnetic conductor," *IEEE Antennas and Wireless Propag. Lett.*, Vol. 15, 950–953, 2016.
18. Li, F., Y. Cui, and R. Li, "A novel broadband AMC surface for lowering the height of planar antennas," *IEEE Int. Symp. On Antennas and Propagation (APSURSI)*, 1110–1111, July 2015.
19. Li, B., W. Hu, J. Ren, and Y. Yin, "Low-profile dual-polarized patch antenna with HIS reflector for base station application," *Journal of Electromagnetic Waves and Applications*, Vol. 28, No. 8, 956–962, 2014.
20. Wang, B., C. Huang, H. Hao, B. Yin, and W. Luo, "Broadband dual-polarized dipole antenna with metallic cylinder for base station," *Electromagnetics*, Vol. 36, No. 8, 515–523, 2016.
21. Sievenpiper, D. F., "High-impedance electromagnetic surfaces," *University of California*, 1999.